Thermal Stability of *n*-Acyl Peroxynitrates

M. KABIR,[1] S. JAGIELLA,[2] F. ZABEL[2]

[1]*Department of Chemistry, Jahangirnagar University, Savar, Dhaka, 1342, Bangladesh*

[2]*Institut für Physikalische Chemie, Universität Stuttgart, Pfaffenwaldring 55, D-70569, Stuttgart, Germany*

Received 19 December 2013; revised 7 May 2014; accepted 7 May 2014

DOI 10.1002/kin.20862
Published online 9 June 2014 in Wiley Online Library (wileyonlinelibrary.com).

ABSTRACT: Peroxynitrates (RO_2NO_2), in particular acyl peroxynitrates (R = R′C(O) with R′ = alkyl), are prominent constituents of polluted air. In this work, a systematic study on the thermal decomposition rate constants of the first five members of the series of homologous $R'C(O)O_2NO_2$ with R′ = CH_3 (=PAN), C_2H_5, *n*-C_3H_7, *n*-C_4H_9, and *n*-C_5H_{11} is undertaken to verify the conclusions from previous laboratory data (Grosjean et al., *Environ. Sci. Technol.* 1994, 28, 1099–1105; Grosjean et al., *Environ. Sci. Technol.* 1996, 30, 1038–1047; Bossmeyer et al., *Geophys. Res. Lett.* 2006, 33, L18810) that the longer chain peroxynitrates may be considerably more stable than PAN. Experiments are performed in a temperature-controlled, evacuable 200 L-photoreactor made from quartz. *n*-Acyl peroxynitrates are generated by stationary photolysis of mixtures of molecular bromine, O_2, NO_2, and the corresponding parent aldehydes, highly diluted in N_2. Thermal decomposition of $R'C(O)O_2NO_2$ is initiated by the addition of an excess of NO. First-order decomposition rate constants k_1 of the reactions $R'C(O)O_2NO_2$ (+M) → $R'C(O)O_2$ + NO_2 (+M) are derived at 298 K and a total pressure of 1 bar from the measured loss rates of $R'C(O)O_2NO_2$, correcting for wall loss of $R'C(O)O_2NO_2$ and several percentages of reformation of $R'C(O)O_2NO_2$ by the reaction of $R'C(O)O_2$ radicals with NO_2. With increasing chain length of R′, k_1(298 K) slightly decreases from 4.4×10^{-4} s^{-1} (R′ = CH_3) to 3.7×10^{-4} s^{-1} (R′ = C_2H_5), leveling off at $(3.4 \pm 0.1) \times 10^{-4}$ s^{-1} for R′ = *n*-C_3H_7, *n*-C_4H_9, and *n*-C_5H_{11}. Temperature dependencies of k_1 were measured for $CH_3C(O)O_2NO_2$ and *n*-$C_5H_{11}C(O)O_2NO_2$ in the temperature range 289–308 K, resulting in the same activation energy within the statistical error limits (2σ) of 0.9 and 1.5 kJ mol^{-1}, respectively. A few experiments on *n*-$C_6H_{13}C(O)O_2NO_2$, *n*-$C_7H_{15}C(O)O_2NO_2$, and *n*-$C_8H_{17}C(O)O_2NO_2$ were also performed, but the results were considered to be unreliable due to strong wall loss of the peroxynitrate and possible complications caused by radical-sinitiated side reactions. © 2014 Wiley Periodicals, Inc. Int J Chem Kinet 46: 462–469, 2014

INTRODUCTION

The oxidation of volatile organic compounds in the troposphere in the presence of the reactive nitrogen oxides NO_x (= NO + NO_2) leads to the production of ozone (O_3) and other secondary photochemical pollutants like peroxynitrates (RO_2NO_2) (see, e.g., [1]). Peroxynitrates with R = alkyl have short thermal lifetimes in the order of seconds at room temperature [2] and can play a role as NO_x reservoirs only at the much lower temperatures of the upper troposphere (see [3] for field measurements of $CH_3O_2NO_2$ in the upper troposphere). Peroxynitrates with R = R′C(O) = acyl exhibit much longer lifetimes in the order of 1 h at

Correspondence to: F. Zabel; e-mail: f.zabel@ipc.uni-stuttgart.de.

Table I Literature Values of k_1 for *n*-Acyl Peroxynitrates at 298 K in 1 bar N_2 or $N_2 + O_2$

Acyl Peroxynitrate	C_n, $n = \ldots$	Grosjean et al. (10^{-4} s^{-1})	IUPAC Review (10^{-4} s^{-1})	JPL Review (10^{-4} s^{-1})
$CH_3C(O)O_2NO_2$	2	3.0[a]	3.3[b] (4.2[c])	3.8[d,e]
$C_2H_5C(O)O_2NO_2$	3	3.4[a]	3.6[b]	3.3[d,e]
n-$C_3H_7C(O)O_2NO_2$	4	3.2[f], 2.7[g]		
n-$C_4H_9C(O)O_2NO_2$	5	1.8[h]		
n-$C_5H_{11}C(O)O_2NO_2$	6	ca. 1.9[i]		
n-$C_6H_{13}C(O)O_2NO_2$	7	ca. 1.0[i]		

[a][20].

[b][10].

[c]Different from the IUPAC evaluation [10], we deduce k(298 K, 1 bar) = 4.2×10^{-4} s^{-1} rather than 3.3×10^{-4} s^{-1} from the original data in Table 2 of [25], claimed to be the basis of the preferred value (see "Comments on Preferred Values" on p. 3906 of [10]). Note that the "high pressure rate constants" cited in [10] are the experimental values at or slightly below 1 bar (different from the heading of the table) except those of Bridier et al. [26] that indeed are the limiting high-pressure value k_∞. From the original data close to 1 bar of Tuazon et al. (4.2×10^{-4} s^{-1}, from Table I in [27]), Bridier et al. (4.1×10^{-4} s^{-1}, from Table I in [26]) and Sehested et al. (4.2×10^{-4} s^{-1}, from Table 2 in [25]) that we consider to be the most comprehensive and reliable data sets, we deduce $k_1 = 4.2 \times 10^{-4}$ s^{-1} at 298 K, 1 bar. It may be noted that the value of Grosjean et al. [20] from our Table I is significantly lower, as was already mentioned in [25].

[d][11].

[e]Calculated for 298 K, 1 bar from falloff parameters for k_{-1} and $K_{eq} = k_{-1}/k_1$.

[f][21]. k_1 was measured at 296 K relative to PAN, the authors present k_1(296 K) = 2.32×10^{-4} s^{-1} using k_1(PAN) = 3.0×10^{-4} s^{-1} at 296 K from Tuazon et al. [27], with k_1(PAN) = 4.17×10^{-4} s^{-1} at 298 K from Ref. [27] we get k_1(*n*-$C_3H_7C(O)O_2NO_2$) = 3.2×10^{-4} s^{-1} at 298 K.

[g][22].

[h][23].

[i][24].

room temperature [4,5] and can serve as reservoirs of NO_x in the atmospheric boundary layer. They participate in the long-range transport of NO_x into remote areas ([6], see also [7] and [8] for more recent work). Hereafter, acyl peroxynitrates with R′ = methyl, ethyl, *n*-propyl, *n*-butyl, etc., are referred to as *n*-acyl peroxynitrates. $CH_3C(O)O_2NO_2$ (PAN, R′ = methyl), the lowest member of this homologous series of peroxynitrates, is an important oxidant in photochemical smog [9]. Extensive kinetic data on the thermal stability exist for PAN in a wide temperature range (see, e.g., [10] and [11]). Higher members of this series of compounds are less abundant than PAN but have also been identified in ambient air: propionyl peroxynitrate (PPN, R′ = ethyl [12]) and *n*-butyryl peroxynitrate (PnBN, R′ = *n*-propyl [13], but see also [14]). Other acyl peroxynitrates already detected in ambient air are *i*-butyryl peroxynitrate (PiBN, R′ = *i*-propyl [14]), methacryloyl peroxynitrate (MPAN, R′ = $H_2C{=}C(CH_3)^\bullet$ [15]), acryloyl peroxynitrate APAN (APAR′ = $H_2C{=}C(H)^\bullet$ [16,17]), PBzN (R′ = phenyl [18]). In atmospheric models, the well-known absolute values of the thermal lifetime of PAN as a function of temperature (Atkinson et al. [10], Sander et al. [11]) are also used for other acyl peroxynitrates (see, e.g., Master Chemical Mechanism (MCM), Saunders et al. [19]) except when more recent kinetic data are available. Experimental data of Grosjean et al. [20–24] at room temperature, however, suggest that the thermal lifetimes of *n*-acyl peroxynitrates generally increase with chain length (by about a factor of 3 when going from acetyl peroxynitrate to *n*-heptanoyl peroxynitrate). Previous experimental data on the first-order rate constants k_1 of the thermal decomposition of several *n*-acyl peroxynitrates,

$$R'C(O)O_2NO_2(+M) \Rightarrow R'C(O)O_2 + NO_2(+M), \quad k_1 \tag{1}$$

are summarized in Table I. In addition, Bossmeyer et al. [28] recently concluded from the observed change of the NO_2 concentration during the reaction of NO_3 with aldehydes in a large environmental chamber that the room temperature value of k_1 may be smaller by as much as a factor of 4 for both $C_2H_5C(O)O_2NO_2$ and *n*-$C_3H_7C(O)O_2NO_2$ compared to the value of PAN.

The data for $C_2H_5C(O)O_2NO_2$ and *n*-$C_3H_7C(O)O_2NO_2$ in Table I are close to the general assumption of the MCM that the thermal stability of other acyl peroxynitrates agrees with that of PAN. Recently, an analysis of the mixing ratios of peroxynitrates measured in two field campaigns by Roberts et al. [29,30] showed that modeling the chemistry based on the MCM mechanism with more recent k_1 values for propionyl peroxynitrate [5] that are 15–20% lower than those of PAN rather than equal to those of PAN has a significant effect on the conclusions drawn concerning the origin of the investigated air masses (anthropogenic vs. biogenic). Qualitatively, the findings of Bossmeyer

et al. [28] are consistent with the trend of k_1 with chain length observed by Grosjean et al. (see Table I). Quantitatively, however, the conclusion of Bossmeyer et al. corresponds to a much stronger decrease of k_1 with chain length than is suggested by the results of Grosjean et al. To resolve these discrepancies, we have addressed in the present work the thermal lifetimes of longer chain, i.e., more complex, *n*-acyl peroxynitrates by measuring k_1 at room temperature for $CH_3C(O)O_2NO_2$, $C_2H_5C(O)O_2NO_2$, *n*-$C_3H_7C(O)O_2NO_2$, *n*-$C_4H_9C(O)O_2NO_2$, and *n*-$C_5H_{11}C(O)O_2NO_2$. For comparison, the temperature dependence of k_1 was measured for both PAN and *n*-$C_5H_{11}C(O)O_2NO_2$ (= *n*-hexanoyl peroxynitrate). In addition, a few experiments were performed for *n*-$C_6H_{13}C(O)O_2NO_2$, *n*-$C_7H_{15}C(O)O_2NO_2$, and *n*-$C_8H_{17}C(O)O_2NO_2$ at room temperature. The results may improve our understanding of the partitioning of reactive nitrogen-oxygen species (= $NO_y \equiv NO + NO_2 + N_2O_5 + HONO + HNO_3 +$ nitrates + peroxynitrates + ...) in the atmosphere (see, e.g., the discussion in [31]).

EXPERIMENTAL

Experiments were performed in a temperature-controlled, evacuable 200-L photoreactor made of quartz (Fig. 1). This reaction chamber is described in more detail in [32]. In brief, peroxynitrates were generated in situ by stationary generation of Br atoms in the presence of the parent aldehyde R′C(O)H, O_2, and NO_2. Product analysis was performed by long-path FT-IR assuming that Beer's law is valid.

In detail, acyl peroxynitrates R′C(O)O_2NO_2 with R′ = CH_3, C_2H_5, *n*-C_3H_7, *n*-C_4H_9, *n*-C_5H_{11}, *n*-C_6H_{13}, *n*-C_7H_{15}, and *n*-C_8H_{17} were prepared in situ at 298 K by photolyzing mixtures of molecular bromine, NO_2, the corresponding aldehydes and 1 bar of $O_2 + N_2$. Bromine atoms are very selective in abstracting aldehydic H atoms, different from the more commonly used Cl atoms that abstract H atoms from the alkyl chain in both the parent aldehydes as well as in the product peroxynitrates in addition to the aldehydic H. The strong selectivity of Br atoms for the aldehydic H atoms is particularly important for the longer chain aldehydes and peroxynitrates. Photolysis mixtures were produced by filling a 2-L evacuated glass bulb with a mixture of Br_2 and R′C(O)H to a certain total pressure in the order of several mbar and transferring the gas into the evacuated chamber, adding 10 or 20 mbar O_2 to the chamber and finally filling up with N_2 to 1 bar. Gas mixing was facilitated by operating a fan for 30 s. Typical initial concentrations (in parentheses, units of 10^{14} molecule cm^{-3}) were R′C(O)H (2), NO_2 (1.5), Br_2 (10), and NO (60). The primary organic products of photolyzing these mixtures with long-wavelength fluorescent lamps (Philips TL 36W/16 yellow, $\lambda > 480$ nm, $\lambda_{max} = 580$ nm) for 30 s were the corresponding acyl peroxynitrates R′C(O)O_2NO_2 (about 5×10^{13} molecule cm^{-3}). The relevant reactions during photolysis are

$$Br_2 + h\nu \Rightarrow 2\,Br \tag{2}$$

$$R'C(O)H + Br \Rightarrow R'CO + HBr \tag{3}$$

$$R'CO + O_2(+M) \Rightarrow R'C(O)O_2(+M) \tag{4}$$

$$R'C(O)O_2 + NO_2(+M) \Leftrightarrow R'C(O)O_2NO_2(+M) \quad (-1,1)$$

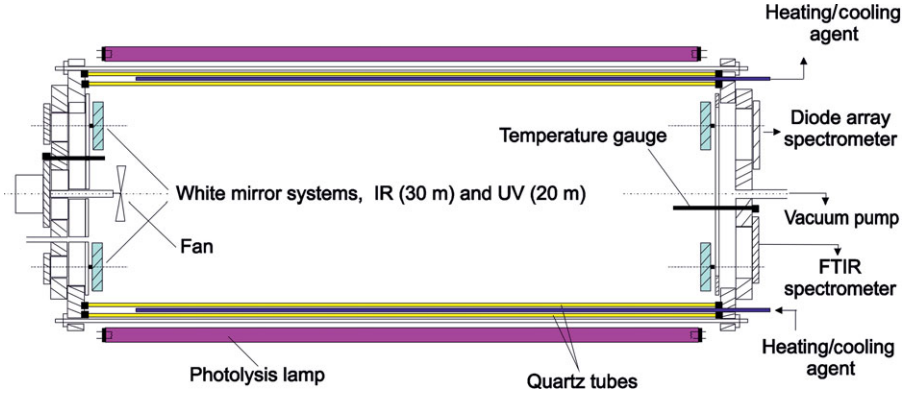

Figure 1 200-L photoreactor from quartz.

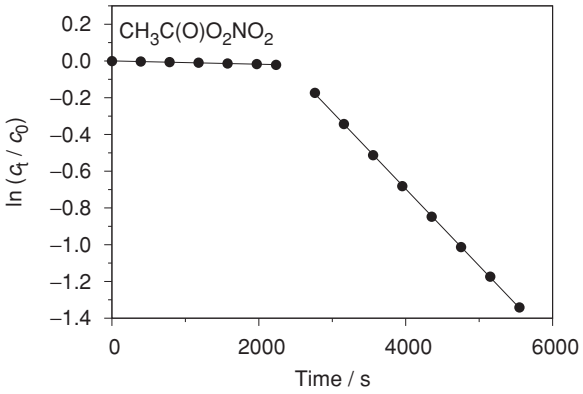

Figure 2 Concentration–time profile for the decomposition of acetyl peroxynitrate (PAN) at 24.7°C in 1 bar of N_2 (each data point represents the average of three spectra).

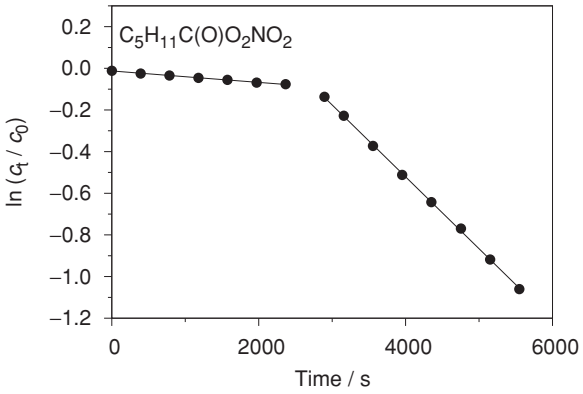

Figure 3 Concentration–time profile for the decomposition of *n*-hexanoyl peroxynitrate at 24.8°C in 1 bar of N_2 (each data point represents the average of three spectra).

In the dark, thermal decomposition of the peroxynitrate was started by adding excess NO to the reaction chamber via gas-tight syringes. Then, the rapid reaction

$$R'C(O)O_2 + NO \Rightarrow R' + CO_2 + NO_2 \qquad (5)$$

withdraws $R'C(O)O_2$ radicals from the equilibrium (–1,1) and prevents the reformation of the peroxynitrate by reaction (–1). Accordingly, the measured first-order loss rate constant of the peroxynitrate is approximately equal to the thermal decomposition rate constant k_1.

Concentrations of R′C(O)H, NO, and NO_2 as well as relative concentrations of $R'C(O)O_2NO_2$ were determined by FT-IR absorption measurements based on calibration spectra. Initially, a background spectrum averaging 256 scans (1 s per scan) in pure nitrogen was measured once a day. In a single experiment, about 60 spectra were taken in the dark after photolysis was terminated. For each spectrum, 128 scans were averaged leading to a time resolution of ca. 2 min. After 40 min in the dark (about one third of the total monitoring time), NO was added to the chamber.

Research-grade chemicals (aldehydes, Br_2, NO, NO_2, O_2, N_2) were used without further purification.

Evaluation of Rate Data and Results

Most of the experiments were performed at 298 ± 0.5 K. Generally, logarithmic plots of the relative peroxynitrate concentrations as a function of time were close to linear both before and after the addition of NO (see Figs. 2 and 3). However, the slope of the first part (before NO addition) was different from zero. This slow linear decay of $\ln[R'C(O)O_2NO_2]$ was assigned to wall loss of the peroxynitrate and subtracted from the slope of the plot after NO addition to give (approximately) the thermal gas phase decomposition rate constant k_1:

$$-\{d(\ln[R'C(O)O_2NO_2])/dt\} = \text{difference of}$$
$$d(\ln(c_t/c_0)/dt)\text{before/after NO addition} \approx k_1 \qquad \text{(I)}$$

where c_t and c_0 are peroxynitrate concentrations at times t and $t = 0$, respectively.

For the low-temperature experiments on *n*-$C_5H_{11}C(O)O_2NO_2$ and the room temperature experiments on *n*-$C_6H_{13}C(O)O_2NO_2$, *n*-$C_7H_{15}C(O)O_2NO_2$, and *n*-$C_8H_{17}C(O)O_2NO_2$, this plot was moderately curved at $t \leq 500$ s, probably due to additional adsorption of the peroxynitrates on the chamber walls, until a constant slope was achieved.

A slight curvature was also observed in these plots after the addition of NO in the low-temperature experiments on PAN and *n*-$C_5H_{11}C(O)O_2NO_2$ and the room temperature experiments on *n*-$C_6H_{13}C(O)O_2NO_2$, *n*-$C_7H_{15}C(O)O_2NO_2$, and *n*-$C_8H_{17}C(O)O_2NO_2$, due to the increase in the ratio $[NO_2]/[NO]$ during the course of the reaction that leads to a competition between reactions (–1) and (5). For the evaluation of k_1, this curvature was approximated by a straight line and the weak slowdown of the loss rate of $R'C(O)O_2NO_2$ during this period was taken into account by using the equation

$$-\{d(\ln[R'C(O)O_2NO_2])/dt\}_{corr} = k_{eff}$$
$$= k_1 \times \{1 + (k_{-1}[NO_2]_{av}/k_5[NO]_{av})\}^{-1} \qquad \text{(II)}$$

Table II Rate Constants k_1 for the Thermal Decomposition of Acyl Peroxynitrates $R'C(O)O_2NO_2$ for $R' = CH_3$, C_2H_5, n-C_3H_7, n-C_4H_9, n-C_5H_{11}, and n-C_6H_{13}

$R'C(O)O_2NO_2$	T_{exp} (°C)	$k_1(T_{exp})$ (10^{-4} s^{-1})	T_2[a] (K)	$k_1(T_2)$[b] (10^{-4} s^{-1})	$k_1(T_2)_{av}$ (10^{-4} s^{-1})
$CH_3C(O)O_2NO_2$	15.5	0.929	289.0	0.984	
	15.5	0.924	289.0	0.978	
	15.5	0.919	289.0	0.973	0.978 ± 0.009[c]
	24.7	4.32	298.0	4.42	
	24.9	4.40	298.0	4.37	
	24.7	4.18	298.0	4.28	
	24.7	4.34	298.0	4.44	
	24.8	4.43	298.0	4.46	4.40 ± 0.13[c]
	35.0	21.8	308.0	21.3	
	35.1	22.2	308.0	21.4	21.4
$C_2H_5C(O)O_2NO_2$	24.9	3.74	298.0	3.71	
	24.7	3.61	298.0	3.69	
	24.6	3.55	298.0	3.69	
	24.7	3.50	298.0	3.58	3.67 ± 0.10[c]
n-$C_3H_7C(O)O_2NO_2$	24.8	3.28	298.0	3.31	
	24.9	3.32	298.0	3.29	
	24.8	3.23	298.0	3.25	
	24.8	3.40	298.0	3.43	3.32 ± 0.13[c]
n-$C_4H_9C(O)O_2NO_2$	24.8	3.42	298.0	3.45	
	24.9	3.38	298.0	3.35	
	24.7	3.37	298.0	3.45	
	24.8	3.41	298.0	3.44	3.42 ± 0.08[c]
n-$C_5H_{11}C(O)O_2NO_2$	15.4	0.713	289.0	0.767	
	15.4	0.695	289.0	0.748	
	15.4	0.701	289.0	0.754	
	15.5	0.659	289.0	0.698	0.742 ± 0.053[c]
	24.7	3.33	298.0	3.41	
	24.8	3.38	298.0	3.41	
	24.7	3.29	298.0	3.37	
	24.8	3.32	298.0	3.35	
	24.8[d]	3.34[d]	298.0[d]	3.37[d]	3.38 ± 0.05[c]
	34.4	16.1	308.0	17.2	
	34.3	15.5	308.0	16.8	
	34.4	15.8	308.0	16.9	16.8 ± 0.5[c]
n-$C_6H_{13}C(O)O_2NO_2$	24.7	(3.23[e])	298.0	(3.31[e])	
	24.6	(3.17[e])	298.0	(3.29[e])	(3.30[e])

[a]Selected fixed temperature representing a group of experiments with $T_{exp} \approx T_2$.

[b]Minor correction from $k_1(T_{exp})$ to $k_1(T_2)$, using the literature value for the activation energy of k_1 for PAN (= 113 kJ mol^{-1}, based on the data collected in Table I of [26]).

[c]2σ error in case there are more than two values of k_1.

[d]In the presence of 2.3×10^{14} molecule cm^{-3} cyclohexane that acts as an OH radical scavenger.

[e]Considered to be less reliable (see the Discussion section).

with $[NO]_{av}$ and $[NO_2]_{av}$ being the mean values of the NO and NO_2 concentrations as measured for the corresponding period of time. Equation (II) is based on the assumption of stationary concentrations for the $R'C(O)O_2$ radical. The correction factor $\{1 + k_{-1}[NO_2]_{av}/k_5[NO]_{av})\}^{-1}$ was between 0.98 and 0.92 under typical reaction conditions such that likewise applying the experimental values of k_{-1} and k_5 for PAN to the longer chain peroxynitrates does not introduce a significant error. The values of k_1 derived from Eq. (II) are listed in Table II. For a better comparison of the rate constants derived from individual experiments at virtually the same but marginally different reaction temperatures T_{exp}, the values of $k_1(T_{exp})$ have been converted to a fixed nearby temperature T_2 (i.e., to 289, 298, or 308 K, respectively), using an Arrhenius expression with $E_a = 113$ kJ mol^{-1} [10,26].

For n-$C_5H_{11}C(O)O_2NO_2$, one experiment was performed in the presence of 2.3×10^{14} molecule cm^{-3} cyclohexane as an OH scavenger. There was no change

in the decomposition rate constant as compared to the experiments without cyclohexane (see Table II, note *d*).

Since the dark decay of peroxynitrates in the absence of added NO (that we assigned to wall loss) potentially may occur from self- or cross-reactions of peroxy radicals, one experiment each was performed for *n*-$C_7H_{15}C(O)O_2NO_2$ and *n*-$C_8H_{17}C(O)O_2NO_2$ with the aim to reduce potential contributions of reaction (6),

$$R'C(O)O_2 + RO_2 \Rightarrow \text{products} \qquad (6)$$

to the first-order loss of $R'C(O)O_2NO_2$. In these experiments, a second portion of NO_2 was added in the middle of the time period before the addition of NO. However, there was no measurable change in the loss rate after the second addition of NO_2.

For $CH_3C(O)O_2NO_2$ and *n*-$C_5H_{11}C(O)O_2NO_2$, a total of eight (for PAN) and five (for *n*-$C_5H_{11}C(O)O_2NO_2$) experiments were performed above and below room temperature (at 34.7 ± 0.4 and 15.5 ± 0.1°C, respectively). These results are also included in Table II. The activation energies from all $k_1(T_{exp})$ values are very similar for both peroxynitrates: 119.9 ± 0.9 kJ mol^{-1} (2σ) for PAN and 121.6 ± 1.5 kJ mol^{-1} (2σ) for *n*-hexanoyl peroxynitrate. The activation energy of PAN from the present work is about 9 kJ mol^{-1} larger than the currently accepted value of about 113 kJ mol^{-1} [10,26], at 1 bar and tropospheric temperatures. Since the scatter of the present data is yet very small, we believe that the discrepancy between our activation energy of k_1 for PAN and the accepted value arises from a small systematic error of the temperature measurements at 289 and 308 K of about 0.5 K leading to an increased activation energy. Thus, the main conclusion from the present experiments is, in accord with previous statements of several research groups (see, e.g., [5,33]), that the activation energies for the gas phase thermal decomposition of *n*-acyl peroxynitrates probably are about the same within statistical error limits.

The first-order rate constants k_1 for the thermal decomposition of *n*-acyl peroxynitrates with $n_C \leq 7$ at 298 K in 1 bar of N_2 are shown in Fig. 4.

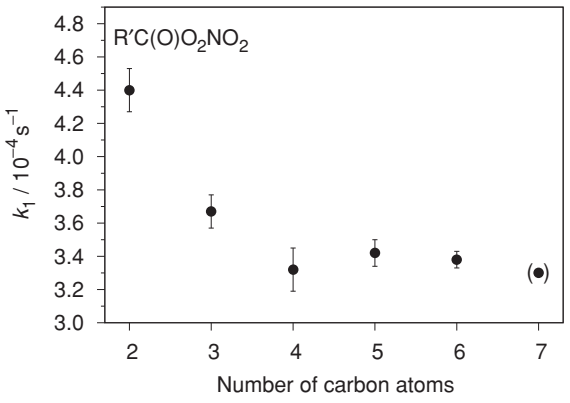

Figure 4 Unimolecular decomposition rate constants k_1 at 298°C in 1 bar N_2 for *n*-acyl peroxynitrates as a function of n_C (= number of carbon atoms, e.g., $n_C = 2$ for PAN).

DISCUSSION

The main conclusion of our work is that in the homologous series of *n*-acyl peroxynitrates, the unimolecular decomposition rate constant in N_2 at atmospheric pressure and a temperature of 298 K slightly decays from PAN with increasing chain length and approaches a nearly constant value for peroxynitrates with four or more C atoms (see Fig. 4). This conclusion is different from the recommendations of the IUPAC panel for k_1 of acetyl peroxynitrate and *n*-propionyl peroxynitrate, where the latter one is slightly larger than the former (see Table I). Qualitatively, our conclusion is in line with suggestions of Grosjean et al. [20–24] and Bossmeyer et al. [28] that the decomposition rate constants of the longer chain *n*-acyl peroxynitrates may be lower by a factor of 3 or 4 as compared to those of PAN. However, we suggest that the rate constants decline by only about 25% from PAN to *n*-butyryl peroxynitrate, leveling off at about 3.4×10^{-4} s^{-1} for the longer chain *n*-acyl peroxynitrates up to *n*-hexanoyl peroxynitrate (Fig. 4).

The present results may be compared with previous data on *n*-acyl peroxynitrates. For PAN, our k_1 at 298 K, 1 bar (4.4×10^{-4} s^{-1}) is in good agreement with the work of Tuazon et al. [27] (4.2×10^{-4} s^{-1}), Bridier et al. [26] (4.1×10^{-4} s^{-1}), and Sehested et al. [25] (4.2×10^{-4} s^{-1}) that we consider to be the most comprehensive and reliable data sets in the literature; see note *c* in Table I. The lower values of Grosjean et al. [20] (see our Table I) are fairly scattered. Our data on *n*-propionyl peroxynitrate (3.7×10^{-4} at 298 K, 1 bar) are in good agreement with previous results on the pressure and temperature dependence of k_1 ([5], 3.5×10^{-4} s^{-1} at 298 K, 1 bar) that were adopted by the IUPAC and JPL reviews [10,11]. For *n*-butyryl peroxynitrate, Grosjean et al. measured both absolute rate constants k_1 from plots of $\ln([PnBN]_t/([PnBN]_0)$ as a function of time [22] and rate constants relative to PAN, from $\ln([PnBN]_t/([PnBN]_0)$ as a function of $\ln([PAN]_t/([PAN]_0)$ [21](see Table I). Converting their

result at 296 K from the relative rate measurements to 298 K using the same source for the rate of the reference reaction (Tuazon et al. [27]), we obtain $k_1(\text{PnBN}) = 3.2 \times 10^{-4}$ s^{-1} at 298 K, in excellent agreement with the present work (3.3×10^{-4} s^{-1}; see Fig. 4 and Table II).

The present results on *n*-acyl peroxynitrates from Fig. 4 may also be compared with literature data on the decomposition rate constants of other acyl peroxynitrates. The value $k_1(298\text{ K}) = 3.5 \times 10^{-4}$ s^{-1} for $H_2C{=}C(CH_3)C(O)O_2NO_2$ ($n_C = 4$) from Roberts and Bertman [33] fits well to the results presented in Fig. 4,* whereas the values from Grosjean et al. for $H_2C{=}C(H)C(O)O_2NO_2$ ($n_C = 3$, $k_1(298\text{ K}) = 3.0 \times 10^{-4}$ s^{-1} [20]), *i*-$C_3H_7C(O)O_2NO_2$ ($n_C = 4$, $k_1(298\text{ K}) = 2.2 \times 10^{-4}$ s^{-1} [22]), and *i*-$C_4H_9C(O)O_2NO_2$ ($n_C = 5$, $k_1(298\text{ K}) = 2.4 \times 10^{-4}$ s^{-1} [23]) are lower by about 20–35%.

In the present work, several photolysis experiments were performed with mixtures of Br_2, NO_2, O_2, N2, and either *n*-heptanal, *n*-octanal, or *n*-nonanal, yielding product spectra with the characteristic peroxynitrate bands. Addition of NO resulted in a decay of these bands with first-order rate constants decreasing with chain length from 3.3×10^{-4} s^{-1} (*n*-$C_6H_{13}C(O)O_2NO_2$) and ca. 3×10^{-4} s^{-1} (*n*-$C_7H_{15}C(O)O_2NO_2$) to ca. 2×10^{-4} s^{-1} (*n*-$C_8H_{17}C(O)O_2NO_2$), i.e., qualitatively in line with the results of Grosjean et al. [20–24] (see Table I) and the conclusions of Bossmeyer et al. [28] but decreasing much more slowly with increasing chain length. However, we considered our results on *n*-$C_6H_{13}C(O)O_2NO_2$, *n*-$C_7H_{15}C(O)O_2NO_2$, and *n*-$C_8H_{17}C(O)O_2NO_2$ to be unreliable for the following reasons:

i. The wall loss rate of *n*-acyl peroxynitrates with $n_C > 6$ strongly increased with chain length arising to about 55% of the total loss rate after NO addition for *n*-$C_8H_{17}C(O)O_2NO_2$, thus allowing to determine the percentage of gas phase decomposition less and less accurately.
ii. Possible interference of the reaction mechanism by OH radicals formed in the $HO_2 + NO$ reaction may strongly increase with increasing chain length due to the abstraction of H atoms from the increasing number of reactive CH_2 groups.
iii. The scatter of the rate constants was considerably stronger for *n*-acyl peroxynitrates with $n_C > 6$ as compared to those for $n_C \leq 6$.

For the above reasons,† the k_1 value measured for *n*-heptanoyl peroxynitrate included in Table II and Fig. 4 is put in parentheses, and the values for *n*-octanoyl and *n*-nonanoyl peroxynitrate are considered to be even more unreliable and are not included in Table II and Fig. 4.

CONCLUSION

The unimolecular decomposition rate constants of the homologous series of *n*-acyl peroxynitrates $R'C(O)O_2NO_2$ at atmospheric pressure and a temperature of 298 K in N_2, starting with PAN ($R' = CH_3$), slightly decays with increasing chain length and approaches a nearly constant value of $(3.4 \pm 0.1) \times 10^{-4}$ s^{-1} for *n*-$C_3H_7C(O)O_2NO_2$, *n*-$C_4H_9C(O)O_2NO_2$, and *n*-$C_5H_{11}C(O)O_2NO_2$. This result supports previous measurements of the thermal stability of PPN relative to that of PAN [5]. Furthermore, it helps to understand the relative abundances of PAN and PPN observed in field measurements by Roberts et al. [29,30]. In general, the present results improve our understanding of the partitioning of reactive nitrogen-oxygen species ($= NO_y \equiv NO + NO_2 + N_2O_5 + HONO + HNO_3 +$ nitrates + peroxynitrates + ...) in the atmosphere.

Dr. M. Kabir thanks the Alexander von Humboldt–Stiftung for a research fellowship.

BIBLIOGRAPHY

1. Finlayson-Pitts, B. J.; Pitts, J. N., Jr. Chemistry of the Upper and Lower Atmosphere; Academic Press: London, 2000.
2. Zabel, F.; Reimer, A.; Becker, K. H.; Fink, E. H. J Phys Chem 1989, 93, 5500–5507.
3. Browne, E. C.; Perring, A. E.; Wooldridge, P. J.; Apel, E.; Hall, S. R.; Huey, L. G.; Mao, J.; Spencer, K. M.; St. Clair, J. M.; Weinheimer, A. J.; Wisthaler, A.; Cohen, R. C. Atmos Chem Phys 2011, 11, 4209–4219.
4. Roberts, J. M. Atmos Environ A 1990, 24, 243–287.

* However, note that $k_1(\text{PAN}) < k_1(\text{MPAN})$ in [33] for 298 K, whereas $k_1(\text{PAN}) > k_1(\text{MPAN})$ for $T > 317$ K, where the error bars for individual data points are significantly lower.

† In addition, unpublished results from our laboratory on the UV spectra of *n*-alkanals [34] have indicated the presence of impurities from unsaturated aldehydes in the purchased samples of *n*-heptanal, *n*-octanal, and *n*-nonanal that are not present in the *n*-alkanals with three to six carbon atoms. These impurities, though very minor, might also affect the chemical mechanisms during thermal decomposition of the corresponding peroxynitrates.

5. Kirchner, F.; Mayer-Figge, A.; Zabel, F.; Becker, K. H. Int J Chem Kinet 1999, 31, 127–144 (Table II).
6. Nielsen, T.; Samuelsson, U.; Grennfelt, P.; Thomsen, E. L. Nature 1981, 293, 553–555.
7. Moxim, W. J.; Levy, H. J., II; Kasibhatla, P. S. J Geophys Res 1996, 101, 12,621–12,638.
8. Li, Q. B.; Jacob, D. J.; Yantosca, R. M.; Munger, J. W.; Parrish, D. D. J Geophys Res 2004, 109, D02313.
9. Finlayson-Pitts, B. J.; Pitts, J. N., Jr. Atmospheric Chemistry: Fundamentals and Experimental Techniques; Wiley: New York, 1986.
10. Atkinson, R.; Baulch, D. L.; Cox, R. A.; Crowley, J. N.; Hampson, R. F.; Hynes, R. G.; Jenkin, M. E.; Rossi, M. J.; Troe J. Atmos Chem Phys 2006, 6, 3625–4055.
11. Sander, S. P.; Finlayson-Pitts, B. J.; Friedl, R. R.; Golden, D. M.; Huie, R. E.; Keller-Rudek, H.; Kolb, C. E.; Kurylo, M. J.; Molina, M. J.; Moortgat, G. K.; Orkin, V. L.; Ravishankara, A. R.; Wine, P. W. JPL Publication 10–6 2011, Evaluation Number 17, Jet Propulsion Laboratory, Pasadena, CA.
12. Singh, H. B.; Salas, L. J. Atmos Environ 1989, 23, 231–238.
13. Grosjean, D.; Williams, E. L., II; Grosjean, E. Environ Sci Technol 1993, 27, 326–331.
14. Roberts, J. M.; Flocke, F.; Stroud, C. A.; Hereid, D.; Williams, E.; Fehsenfeld, F.; Brune, W.; Martinez, M.; Hard, H. J Geophys Res 2002, 107, 4554.
15. Grosjean, D.; Williams, E. L., II; Grosjean, E. Environ Sci Technol 1993, 27, 110–121.
16. Tanimoto, H.; Akimoto, H. Geophys Res Lett 2001, 28, 2831–2834.
17. Roberts, J. M.; Jobson, B. T.; Kuster, W.; Goldan, P.; Murphy, P.; Williams, E.; Frost, G.; Riemer, D.; Apel, E.; Stroud, C.; Wiedinmyer, C.; Fehsenfeld, F. J Geophys Res 2003, 108, D16, 4495.
18. Fung, K.; Grosjean, D. Sci Total Environ 1985, 46, 29–40.
19. Saunders, S. M.; Jenkin, M. E.; Derwent, R. G.; Pilling, M. J. Atmos Chem Phys 2003, 3, 161–180.
20. Grosjean, D.; Grosjean, E.; Williams, E. L., II J Air Waste Manage Assoc 1994, 44, 391–396.
21. Grosjean, D.; Williams, E. L., II; Grosjean, E. Int J Chem Kinet 1994, 26, 381–387.
22. Grosjean, D.; Grosjean, E.; Williams, E. L., II Res Chem Intermed 1994, 20, 447–461.
23. Grosjean, D.; Grosjean, E.; Williams, E. L., II Environ Sci Technol 1994, 28, 1099–1105.
24. Grosjean, E.; Grosjean, D.; Seinfeld, J. H. Environ Sci Technol 1996, 30, 1038–1047.
25. Sehested, J.; Christensen, L. K.; Møgelberg, T.; Nielsen, O. J.; Wallington, T. J.; Guschin, A.; Orlando, J. J.; Tyndall, G. S. J Phys Chem A 1998, 93, 1779–1789.
26. Bridier, I.; Caralp, F.; Loirat, H.; Lesclaux, R.; Veyret, B.; Becker, K. H.; Reimer, A.; Zabel, F. J Phys Chem 1991, 95, 3594–3600.
27. Tuazon, E. C.; Carter, W. P. L.; Atkinson, R. J Phys Chem 1991, 95, 2434–2437.
28. Bossmeyer, J.; Brauers, T.; Richter, C.; Rohrer, F.; Wegener, R.; Wahner, A. Geophys Res Lett 2006, 33, L18810.
29. Roberts, J. M.; Flocke, F.; Chen, G.; de Gouw, J.; Holloway, J. S.; Huebler, G.; Neuman, J. A.; Nicks, D. K., Jr.; Nowak, J. B.; Parrish, D. D.; Ryerson, T. B.; Sueper, D. T.; Warneke, C.; Fehsenfeld, F. C. J Geophys Res 2004, 109, D23S21.
30. Roberts, J. M.; Marchewka, M.; Bertman, S. B.; Sommariva, R.; Warneke, C.; de Gouw, J.; Kuster, W.; Goldan, P.; Williams, E.; Lerner, B. M.; Murphy, P.; Fehsenfeld, F. C. J Geophys Res 2007, 112, D20306.
31. Day, D. A.; Dillon, M. B.; Wooldridge, P. J.; Thornton, J. A.; Rosen, R. S.; Wood, E. C.; Cohen, R. C. J Geophys Res 2003, 108, 4501.
32. Libuda, H. G.; Shestakov, O.; Theloke, J.; Zabel, F. Phys Chem Chem Phys 2002, 4, 2579–2586.
33. Roberts, J. R.; Bertman, S. B. Int J Chem Kinet 1992, 24, 297–307.
34. Shestakov, O.; Libuda, H. G.; Zabel, F. In Abstract Book of the 98th Bunsentagung; Dortmund, Germany, 1999.